MARMARA
MEDICAL JOURNAL

Original Article

https://dergipark.org.tr/tr/pub/marumj

Low-dose LPS and calorie restriction combined therapy for pancreatic ductal adenocarcinoma: an *in vitro* and *in vivo* study

Alisa Bahar BEYDOGAN[1], Basak ISILDAR[2], Zeynep Mine COSKUN YAZICI[3], Meral KOYUTURK[2], Sema BOLKENT[1]

[1] Department of Medical Biology, Cerrahpaşa Faculty of Medicine, Istanbul University-Cerrahpaşa, Istanbul, Türkiye.
[2] Department of Histology and Embryology, Cerrahpaşa Faculty of Medicine, Istanbul University-Cerrahpaşa, Istanbul, Türkiye.
[3] Department of Molecular Biology and Genetics, Faculty of Arts and Sciences, Demiroglu Bilim University, Istanbul, Türkiye
Corresponding Author: Sema Bolkent
E-mail: bolkent@iuc.edu.tr

Submitted: 09.03.2024 **Accepted:** 04.09.2024

ABSTRACT

Objective: This study aimed to evaluate the therapeutic effects of lipopolysaccharide (LPS) on Panc02 cells since LPS is an inflammatory agent with the potential to activate the immune system and reorganize the tumor microenvironment. Moreover, calorie restriction (CR) has been investigated in combination with LPS as a prospective adjuvant intervention for cancer therapy.

Materials and Methods: Panc02 cells were cultured in two distinct media with low and high-glucose concentrations, and cell viability was investigated after applying varying doses of LPS to culture media. The *in vivo* effects of LPS and CR were investigated on the mice subcutaneous pancreatic ductal adenocarcinoma (PDAC) tumor model in terms of tumor mass, histological examination, mRNA expression profiles, and biochemical parameters.

Results: The lowest cell count was detected in the cells treated with 10 µg/ml LPS in low-glucose environments *in vivo*. Tumor mass significantly decreased in the P+LPS+CR group *in vivo*. The mRNA expression analysis of tumor tissues indicated that P+LPS+CR acts through NF-κB, JNK, and IL-6 signaling pathways.

Conclusion: Lipopolysaccharide alone is insufficient to show therapeutic effects, but it can inhibit tumor development by acting on NF-κB and JNK pathways when combined with CR. This study gives insight into developing new treatment options for PDAC.

Keywords: Panc02, Lipopolysaccharide, Calorie restriction, Subcutaneous pancreatic ductal adenocarcinoma model, Cancer

1. INTRODUCTION

Pancreatic ductal adenocarcinoma (PDAC) is a highly aggressive and lethal neoplasm. Although, it accounts for just 3% of newly diagnosed cancer cases, it ranks as the third leading cause of cancer-related deaths worldwide. Projections suggest that by 2030, it will become the second leading cause of cancer-related deaths in the United States [1]. Due to the difficulty of early diagnosis and limited treatment options, the 5-year survival rate is for PDAC only 7% [2]. Conventional treatments like chemotherapy and radiotherapy have shown little success in improving this survival rate. Therefore, it is necessary to understand carcinogenesis, progression, metastasis, tumor microenvironment, and the molecular pathways involved in these steps and develop appropriate treatment strategies [3].

Lipopolysaccharide (LPS) is the predominant constituent in the outer membrane of gram-negative bacteria. It consists of a poly – or oligosaccharide district attached in the outer bacterial membrane by a particular carbohydrate lipid moiety named lipid A, which serves as the principal immunostimulatory region within LPS. It is a powerful stimulant of innate immunity in humans and other eukaryotic organisms [4]. LPS performs this function by stimulating monocytes/macrophages, which play crucial roles in protecting the host cell against infections and tissue damage. This stimulation occurs via the Toll-like receptor 4 (TLR4), a type-1 transmembrane protein. Thus, important mediators of LPS signaling are activated, including mitogen-activated protein kinase (MAPK), nuclear factor Kappa-B (NF-κB), and activator protein-1 (AP-1) [5]. Initiating

How to cite this article: Beydogan AB, Isildar B, Coskun Yazici ZM, Koyuturk M, Bolkent S. Low-dose LPS and calorie restriction combined therapy for pancreatic ductal adenocarcinoma: an *in vitro* and *in vivo* study. Marmara Med J 2025;38(1): 15-23 doi: 10.5472/marumj.1627620

ISSN: 1309-9469

http://doi.org/10.5472/marumj.1627620
Marmara Med J 2025;38(1): 15-23

a sequence of signaling events leads to an elevation in the synthesis of inflammatory agents, including proinflammatory cytokines like TNF-α, interleukin (IL-1), and IL-6, as well as nitric oxide and eicosanoids [6]. These substances contribute to tissue harm and widespread inflammation [7].

Calorie restriction (CR) is a diet that includes a 20-40% decline in total energy intake but allows adequate essential nutrients [8]. Pre-clinical studies have demonstrated that it increases life expectancy and delays the initiation of age-related conditions, such as type 2 diabetes, cardiovascular diseases, cancer, and neurodegenerative disorders [9]. The metabolic effects of CR are actively regulated processes aimed at reducing oxidative stress, triggering a robust defense program involving multiple metabolic pathways [10]. When calorie intake is reduced, the organism undergoes health-promoting changes. These changes include increased apoptosis in tumors, decreased angiogenesis, adjustments in systemic signals such as insulin-like growth factor (IGF)-1, improved insulin sensitivity, and alterations in metabolic and inflammatory mechanisms [9]. Recent research using animal models has demonstrated that CR reduces cancer occurrence and effectively slows its progression. Various signaling pathways cooperate and cross-communicate to control carcinogenesis under CR conditions. CR-mediated anticancer activity is known to involve IGF 1/PI3K/AKT, mTOR, NF-κB, and AMPK signaling pathways [11, 12] showed that multiple fasting cycles could potentially modify or increase the efficacy of chemotherapeutic agents in the treatment of different cancer cells, such as glioma, breast cancer, neuroblastoma, and melanoma [13].

Therefore, the synergetic effects of using CR in addition to current and newly developed treatment methods should be investigated [14]. So, this study aimed to investigate the effects of LPS and CR applications on Panc02 cells *in vitro* and *in vivo* subcutaneous tumor models and evaluate the therapeutic approaches to PDAC.

2. MATERIALS and METHODS

Cell culture and dosing experiments

Murine pancreatic adenocarcinoma cell line Panc02 has been generously donated by Dr. Christine Hackbarth and Dr. Lars Ivo Partecke from the Department of Surgery, University of Greifswald, Germany. After receiving the cells, the mycoplasma test was performed at the Department of Medical Microbiology, Cerrahpasa Medical Faculty, and the cells were detected as negative for mycoplasma. Panc02 cells were cultured at 37°C, under a humidified atmosphere with 5% CO_2. They expanded in Dulbecco's Modified Eagle's Medium/Nutrient Mixture F-12 (DMEM/F12 Sigma, USA, D0697) supplemented with 10% (v/v) Fetal Bovine Serum (FBS: Hyclone, UK) and 1% penicillin/streptomycin (Hyclone, UK).

The experiments to determine the lethal dose of LPS for Panc02 cells were conducted in media with low (calorie restriction mimetic media) and high glucose concentrations, 1.5 g/L and 4.0 g/L, respectively (DMEM/F12 Sigma, USA, D6046 and 5796). These experiments were repeated three times. The dosing experiments were performed in six-well plates, and $5x10^5$ cells were seeded per well for initial. LPS (Sigma-Aldrich, USA, L8274) concentration has been determined as 1, 5, 10, 25, and 50 µg/ml for 24 hours of incubation, and as a control group, LPS has not been applied to one of the wells. Cell viability was analyzed through trypan blue staining, and the total count of viable cells was determined by manually counting them using a hemocytometer under the Olympus IX71 inverted microscope (Olympus, Tokyo, Japan). Based on the results, a dose of 10 µg/mL LPS was selected for use in the *in vitro* experiments.

Immunocytochemistry

Panc02 cells were seeded on coverslips placed on six-well plates and cultured in low and high-glucose media. When the cells reached 80% confluency, 10 µg/ml LPS was added to the medium. Untreated cells served as control groups. After 24 hours of incubation, the coverslips were fixed with cold methanol. Then, the coverslips were washed three times with cold phosphate-buffered saline, and the immunocytochemistry step started. Initially, non-specific binding was prevented by blocking with 5% bovine serum albumin (BSA). Subsequently, the coverslips were subjected to an overnight incubation at 4°C with the primary antibody [anti-caspase-3 (Santa Cruz, California, USA) was used at a 1:100 dilution]. Next, the cells were treated with the biotinylated-secondary antibody (SHP125; ScyTek, West Logan, Utah), followed by the streptavidin-peroxidase conjugate. Aminoethyl carbazole (Invitrogen, California, United States) was used as the chromogen. The samples have been counterstained with Mayer's hematoxylin (ThermoFisher, Waltham, MA, USA) and examined by light microscopy (Olympus BX61) [15].

In vivo Panc02 tumor model

In this study, 10 – to 13-week-old C57BL/6 male mice obtained from the Experimental Application and Research Center, Bezmialem Foundation University, were used. All mice were kept in standard conditions according to the Regulation of Animal Research Ethics in Turkey. The ethical approval was granted by the Bezmialem Foundation University, Laboratory Animals Local Ethics Committee (Project number 2017/190, İstanbul, Turkey). A subcutaneous tumor model was generated in those animals by the subcutaneous injection of Panc02 cells ($1x10^6$) from the upper part of their left legs [16]. The experimental groups, each consisting of n=8 mice, were determined [17] and are represented in Table I. The experimental process was planned as an average of 15 days for tumor development, followed by 14 days of low-dose LPS application (7 days 0.5 mg/kg followed by 7 days 1 mg/kg LPS). Throughout the experiment, animals on a normal diet consumed an average of 5 g of feed per day, whereas those subjected to a 40% CR consumed 3 g daily [18]. Details of the experimental groups are provided in Table I. The tumor tissue of each animal was measured with a digital caliper at the end of the experiment.

http://doi.org/10.5472/marumj.1627620
Marmara Med J 2025;38(1): 15-23

Table I. *The experimental groups (n=8)*

Panc02 Group (P):	The animals were sacrificed two weeks after the tumor diameter exceeded 60 mm^3 while being fed an average of 5 g of feed per day throughout the experiment.
Panc02+LPS Group (P+LPS):	After the tumor diameter exceeded 60 mm^3, LPS was administered to the animals intraperitoneally (0.5 mg/kg for seven days, followed by 1 mg/kg for the second seven days). The animals were fed an average of 5 g of feed per day throughout the experiment.
Panc02+LPS+Calorie Restriction Group (P+LPS+CR):	After the tumor diameter exceeded 60 mm^3, LPS was administered to the animals intraperitoneally (0.5 mg/kg for seven days, followed by 1 mg/kg for the second seven days). The animals were fed an average of 3 g of feed per day throughout the experiment.

LPS: Lipopolysaccharide

Histological Analysis

The tumor tissues were fixed with a 10% neutral buffered formalin solution, dehydrated with ethanol, and embedded in paraffin. 4-µm sections were taken from paraffin blocks and stained with Masson's trichrome stains for histological examinations. Following the staining process, the nuclei exhibit a dark red, the cytoplasm appears light red, and the connective tissue is distinctly stained green due to the collagen it contains. The sections were examined with an Olympus BX61 digital microscope (Olympus, Tokyo, Japan) attached to a computerized digital camera (DP72) (Olympus, Tokyo, Japan).

Real-Time PCR Assay

For real-time polymerase chain reaction (qRT-PCR), cDNA was synthesized from 200 ng of RNA. NF-κβ, interleukin-6 (IL-6), and c-Jun N-terminal kinase (JNK) gene regions were investigated. β-Actin was used as the housekeeping gene (Table II). 2 µl of cDNA was placed in a 96-well plate, and the reaction mix (SYBR Green), primers, and nuclease-free water were added onto it, resulting in a total volume of 20 µl. For the negative control, RNAse-free water was substituted for the sample. The plate was carefully covered with occlusive film. The plate was placed in the BioRad CFX96 Real-time PCR device, and PCR reactions were performed with the following reaction profile: 95°C for 3 minutes, 95°C for 15 seconds, 59°C for 25 seconds, 72°C for 30 seconds for 40 cycles.

Table II. *Primer details*

mRNA	Sequence (from 5' to 3')
NF-κB	Forward - 5'CCGGGAGCCTCTAGTGAGA 3' Reverse - 5'CATTTGTGACCAACTGAACGA 3'
JNK	Forward - 5'GATTTTGGACTGGCGAGGACT 3' Reverse - 5'TAGCCCATGCCGAGAATGA 3'
IL-6	Forward - 5'ACCACCCACAACAGACCAGT 3' Reverse - 5'TTTGGAAGCATCCATCATTTC 3'
B-Actin	Forward - 5'GGGAATGGGTCAGAAGGACT 3' Reverse - 5'TTTGATGTCACGCACGATTT 3'

mRNA: Messenger ribonucleic acid, NF-κB Nuclear - factor - Kappa B, JNK: c-Jun N-terminal kinase, IL-6: Interleukin-6, B-Actin: Beta-actin

Biochemical analysis

Tumor tissue extracted from the animals was homogenized in the physiological saline solution for biochemical analysis. The total protein in the homogenate was quantified according to the Bradford method [19]. Subsequently, the biochemical analyses given below were performed on the diluted homogenate.

– ***Catalase (CAT) Activity:*** CAT activity was determined using the Aebi method [20], where diluted tumor tissue homogenate was mixed with 50 mM phosphate-buffered saline (pH 7.0) and 30 mM H_2O_2. Absorbance readings were taken at 240 nm, and the results were expressed as U/mg.

– ***Malondialdehyde (MDA) level:*** MDA, a peroxidation product resulting from fatty acid reactions with free radicals, was quantified using the Ledwozyw method [21]. Briefly, 1 ml of 30% trichloroacetic acid (TCA) solution, 200 µl of 5 M hydrochloric acid (HCl) solution, and 1.5 ml of 0.75% thiobarbituric acid solution were added to 250 µl of tissue samples. After vortexing, the mixture was incubated for 15 minutes, followed by boiling at 95-100°C for 40 minutes. The pink solution obtained was then centrifuged, the supernatant read at 532 nm, and the results were expressed as nmol/mg.

– ***Glutathione (GSH) level:*** GSH levels, an antioxidant marker, were quantified using the Beutler method [22]. Precipitation solution (containing glacial metaphosphoric acid, EDTA-Na_2HPO_4, and NaCl) was mixed with tissue homogenate, vortexed for 5 minutes, and centrifuged at 4000 rpm. The supernatant was collected and mixed with secondary sodium phosphate (0.3 M) and DTNB (prepared in 1% sodium citrate solution). After a 5-minute incubation at room temperature, absorbance readings at 412 nm were taken, and GSH levels were expressed as nmol/mg relative to tissue protein concentration.

– ***Superoxide Dismutase (SOD) level:*** SOD activity, an antioxidant marker, was quantified using Sun method [23]. Tumor tissue homogenate was mixed with absolute alcohol and chloroform, vortexed, and then centrifuged at 10000 rpm at +4°C for 20 minutes. The resulting supernatant was combined with a substrate solution at pH 10.2 (containing Na_2CO_3, Na_2EDTA, NBT, and BSA) and xanthine oxidase (XO), followed by a 20-minute incubation at room temperature in the dark. $CuCl_2.2H_2O$ was added to stop the reaction, and absorbance was measured at 560 nm. SOD activity, expressed as U/mg was calculated based on the assumption that 1 unit of SOD activity inhibits XO activity by 50%.

– ***Protein Carbonyl (PCO) level:*** PCO levels, an oxidative stress marker, were determined using the Reznick and Packer method [24]. Tumor tissue homogenate was mixed with a 10 mM 2,4-dinitrophenylhydrazine solution prepared in 2.5 M HCl and incubated for 1 hour in the dark, with periodic vortexing every 15 minutes. To precipitate protein, 20% TCA was added, vortexed, and then centrifuged at 5000 g for 5 minutes at +4°C. The resulting pellet was washed with 10% TCA and centrifuged again. The pellets were washed three times with ethanol: ethyl acetate (1:1). After washing, 6M guanidine-HCl solution was added, vortexed, and dissolved. It was then incubated at 37°C for 10 minutes to dissolve all particles, and

absorbance was measured at 560 nm. PCO concentration was expressed as nmol/mg.

Statistical Analysis

SPSS.21 and Graphpad 5 software programs were used for statistical analysis. Normality was evaluated with the Shapiro-Wilk test. One-way ANOVA determined multiple comparisons of normally distributed variables, and the Tukey test determined pairwise comparisons. Kruskal Wallis and Mann-Whitney U tests were used for non-normally distributed variables. A value of p<0.05 was considered significant.

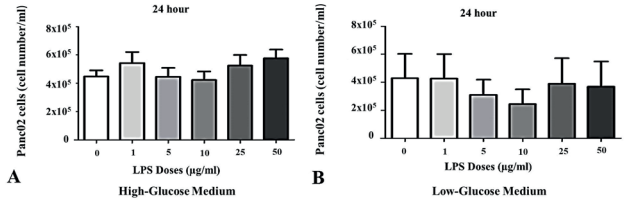

Figure 1: *The effect of lipopolysaccharide (LPS) on Panc02 cells. Viable cell numbers were assessed following the application of different doses of LPS to Panc02 cells in media containing high glucose (HG) (A) and low glucose (LG) (B). The data were presented as mean ± SEM.*

3. RESULTS

The effect of LPS on Panc02 cells and PDAC tumor

The Panc02 cells were cultured for 24 hours with different LPS concentrations in high (Figure 1A) and low (Figure 1B) glucose concentrations. As a result of the cell viability assay, the lowest cell count was detected in the cells treated with 10 µg/ml LPS in low glucose environments. *In vitro* experiments showed that after 24 hours of LPS administration to Panc02 cells, low glucose media mimicking the calorie restriction pattern had fewer cells than high glucose media receiving the same dose. The ratio of cells displaying caspase-3 positivity exhibited a significant difference among the groups ($p < 0.05$). A significant increase in caspase-3 immunoreactivity was observed in cells of the high glucose+LPS group compared to the high glucose control group ($p < 0.05$). Interestingly, in cells cultured in the low-glucose medium, the caspase-3 immunoreactivity in the LPS group was lower than in the control group ($p < 0.05$) (Figure 2A-E). Tumor follow-up results in *in vivo* experiments showed a significant reduction of tumor mass in the Panc02 (P)+LPS+CR group ($p <0.01$). The reduction in the tumor size was highly significant when the P+LPS+CR group was compared with the P group ($p <0.001$). A significant difference was observed between P+LPS and P+LPS+CR groups ($p < 0.01$) and it was determined that CR application, in addition to LPS, caused significant tumor shrinkage. There was no statistically significant difference between the P+LPS and the P groups (Figure 3A). Tumor mass evaluation showed that the lowest tumor mass was in the P+LPS+CR group, which was statistically significant. Similar to the tumor size measurements, no significant reduction was observed in the P+LPS group compared to the P group. When the P+LPS+CR group was compared with the P and P+LPS groups, a significant decrease was seen in tumor mass ($p < 0.001$, $p < 0.05$, respectively), (Figure 3B). According to these findings, the combination of LPS and 40% CR in the PDAC model has been shown to have significant regressive effects on tumor development. The fact that the weight and the size reduction in the P+LPS groups were not statistically significant compared to the control group indicates the impressive effect of CR applied as a support for the therapeutic use of LPS. These results demonstrate that LPS+CR administration significantly suppresses tumor growth in the *in vivo* Panc02 subcutaneous tumor model.

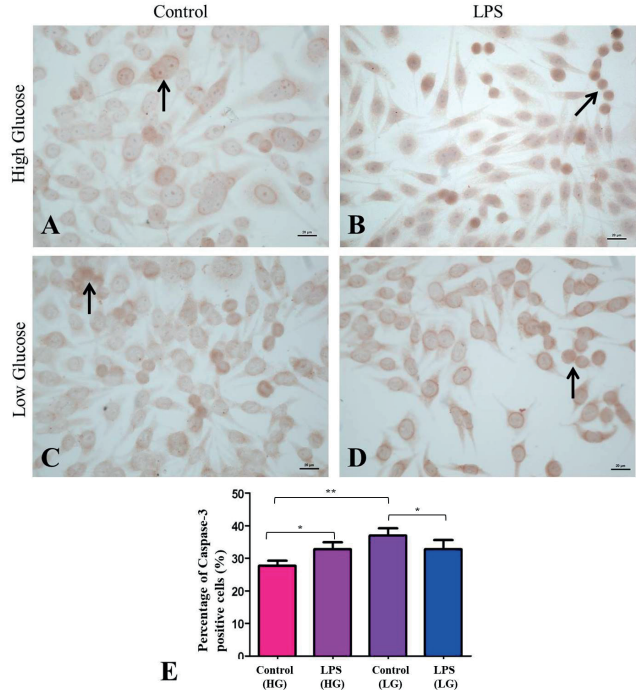

Figure 2: *Caspase-3 immunoreactivity in Panc02 cells (arrows). High glucose (HG) control group (A). HG + LPS group (B). Low Glucose (LG) control group (C). LG + LPS group (D). Percentages of caspase-3 positive cells (%) (E). *p<0.05, **p<0.01. The data were expressed as mean ± SEM.*

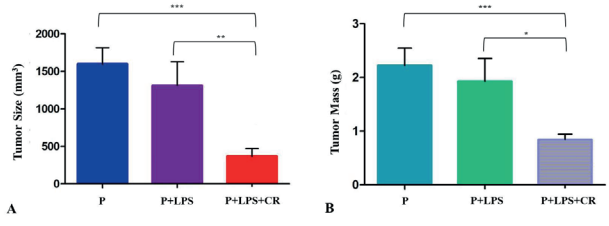

Figure 3: *Tumor size and mass measurements. Tumor size measurements (A). Tumor mass measurements (B). *p<0.05, **p<0.01, ***p<0.001. The data were expressed as mean ± SEM.*

http://doi.org/10.5472/marumj.1627620
Marmara Med J 2025;38(1): 15-23

Histological Analysis

According to the light microscopic examination, connective tissue was decreased in the P+LPS and P+LPS+CR groups compared with the P group, and the decrease was prominent in the P+LPS+CR group. Ductal-shaped structures were noticed in all tumor tissues (Figure 4A-C).

The messenger ribonucleic acid (mRNA) expression profiles for NF-κB, JNK, and IL-6 in tumor tissues

The mRNA expressions of NF-κB, JNK, and IL-6 are represented in Figure 5. NF-κB expression levels were similar in the P and the P+LPS groups. When the P+LPS+CR and P+LPS groups were compared, it has been shown an increase in the P+LPS+CR group ($p < 0.05$) (Figure 5A). When JNK expression levels were analyzed, it was determined that there was a significant increase in both the P+LPS and P+LPS+CR groups according to the P group ($p < 0.05$), (Figure 5B). In addition, IL-6 mRNA expression levels were increased in both the P+LPS and the P+LPS+CR groups compared to the P group ($p < 0.05$). The highest expression was detected in the P+LPS+CR group (Figure 5C).

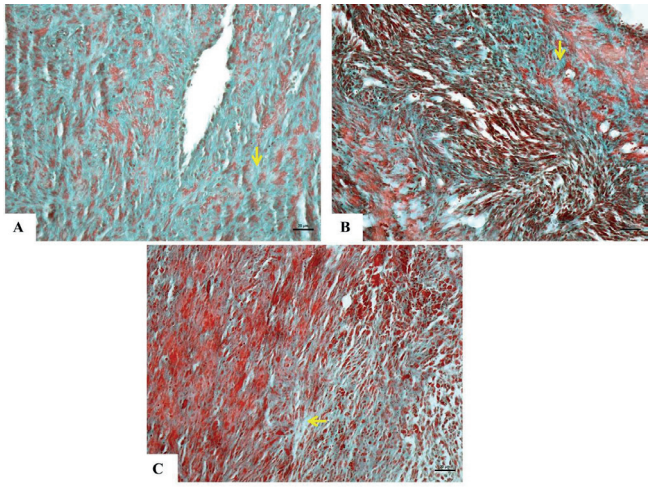

Figure 4: *Histological appearance of the tumor tissues. Panc02 (P) group (A). Panc02 + lipopolysaccharide (P+LPS) group (B). Panc02 + LPS + calorie restriction (P+LPS+CR) group (C). Arrow: Collagen fibers of connective tissue. x20, Masson's Trichrome.*

Biochemical analysis for CAT, GSH, SOD, MDA and PCO levels in tumor tissue

When the tumor tissue was examined for antioxidant status biochemically, CAT enzyme activity was higher in the treatment groups than in the P group. However, no significant difference was found between the groups (Figure 6A). GSH and SOD levels were not changed significantly in the treatment groups (Figure 6B-C). Oxidative stress status was examined by MDA and PCO levels in tumor tissues. There was no significant difference between the groups when tumor tissues were evaluated at the MDA and PCO levels, respectively (Figure 6D-E).

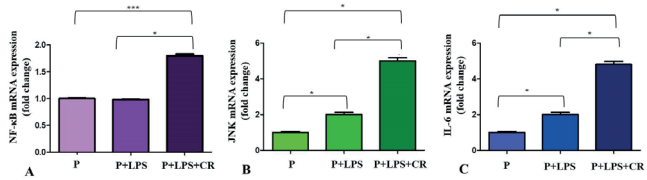

Figure 5: *The mRNA profiles of the tumor tissues. The mRNA expressions of NF-κB (A), JNK (B), and IL-6 (C). $^{*}p<0.05$, $^{***}p<0.001$. The data were expressed as mean ± SEM.*

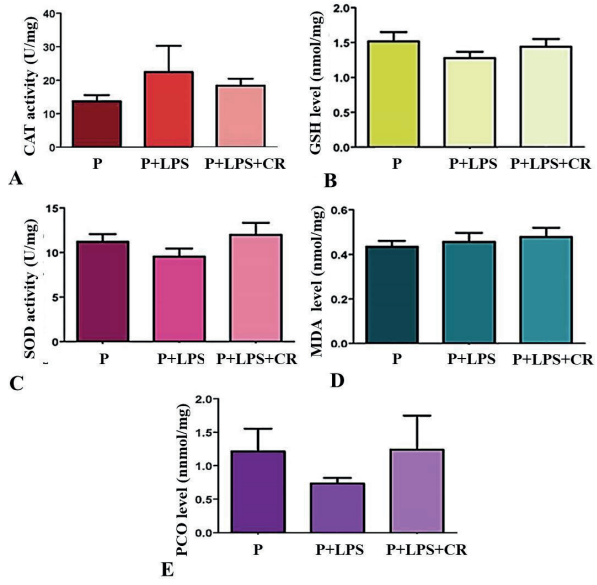

Figure 6: *Biochemical Analysis. Catalase (CAT) activity (A), glutathione (GSH) level (B), superoxide dismutase (SOD) activity (C), malondialdehyde (MDA) level (D), and protein carbonyl (PCO) level (E) in the tumor tissues. The results were expressed as mean ± SEM.*

4. DISCUSSION

The study primarily investigated the impacts of LPS and CR on PDAC *in vitro* and *in vivo*. These effects were shown through the cell viability, inflammation, and oxidative stress pathways. LPS has a dual effect on cancer progression. It promotes the proliferation and migration of cancer cells at high doses. On the other hand, it has been reported that its use at low doses can suppress tumor cell progression by having the opposite effect [25, 26]. It is known that LPS can cause sepsis in high doses. Still, in recent years, it has begun to be investigated that low-dose LPS treatment may provide potential benefits, especially in cancer and autoimmune diseases [27]. Beyond the therapeutic promise of LPS, the concern over potential side effects leading to sepsis emerges as a limiting factor in studies involving this agent. Nevertheless, the administration of low doses of LPS to humans, along with ongoing adjustments based on administration routes,

http://doi.org/10.5472/marumj.1627620
Marmara Med J 2025;38(1): 15-23

suggests a demonstrated therapeutic applicability [28–31]. This evolving understanding highlights the increasing significance of effectively utilizing LPS in preclinical studies. Calorie restriction (CR), which is used in addition to LPS in our study, emerges as a noteworthy adjunctive therapy. A study showed that CR applied in pancreatic cancer caused a diet-related change in the tumor microenvironment by reducing the enzyme activity that converts saturated fatty acids to unsaturated fatty acids, which could suppress tumor development [32]. In another research by Lashinger et al., CR has been shown to delay the progression of PanIN lesions to PDAC and reduce pancreatic desmoplasia and metastases [33]. CR applications can be applied to humans in various ways, including periodic fasting, fasting-mimicking diets, and dietary restriction before chemotherapy and similar treatments [34]. Considering the positive effects of CR on tumor cells and tumor microenvironment, as well as its properties of protecting normal cells and increasing drug permeability [35], it was planned to be used as a supportive treatment to increase the effect of LPS in the Panc02 tumor model in this study.

According to *in vitro* results, the low-glucose medium, which mimics CR, had fewer cell counts than the high-glucose medium with the same LPS dose after 24 hours of applying LPS to Panc02 cells. Based on the findings from caspase-3 immunostaining, the administration of LPS led to a significant increase in apoptosis in cells cultured in the high-glucose medium. Additionally, there was a noteworthy increase in the apoptosis rate in Panc02 cells cultured in a low-glucose environment, even without LPS treatment. These results collectively demonstrate that both LPS administration and CR decelerate the growth of tumor cells *in vitro*. Upon evaluating the *in vivo* outcomes, a notable reduction in both tumor size and mass was evident in the P+LPS+CR group. Interestingly, compared to the control group, the lack of statistical significance within the P+LPS groups underlines the remarkable impact of CR when applied as a supportive therapy in addition to LPS therapy. These findings collectively emphasize the significant tumor-suppressive effects of the LPS+CR administration in the *in vivo* Panc02 subcutaneous tumor model. Research suggests that although applying LPS has been associated with increased proliferation and migration in prostate and colorectal cancer cells [36, 37], there is an indication that at lower doses, LPS could prevent tumor progression [25]. This potential effect is attributed to the impact of LPS dose on various macrophage functions, potentially regulating inflammatory changes in tissues and the tumor microenvironment. Consequently, the prospect of employing low-dose LPS therapy holds promise in advancing treatments for cancer and autoimmune diseases by mitigating chronic inflammation. However, in our study, LPS alone did not exhibit the anticipated effectiveness in reducing tumor size. This effect was only observed with the CR application. Reduced calorie intake triggers health-promoting changes within the organism, including enhanced apoptosis within tumors, reduced angiogenesis, modulation of systemic signals, insulin sensitivity, and metabolic and inflammation mechanisms [9]. Besides, CR has a significant impact not only on cancer cells but also on the tumor microenvironment. It enhances drug delivery, reduces the availability of growth factors for cancer cells, and modulates inflammation and oxidative stress within the tumor microenvironment. These effects contribute to the potential efficacy of CR in cancer treatment, and its use as a supportive treatment gains importance, especially thanks to its drug permeability-increasing effect [10]. According to our results, 40% calorie restriction showed a significant beneficial effect together with LPS. Therefore, as demonstrated in our study, the synergistic effects of using calorie restriction in addition to existing and newly developed treatment methods have gained importance.

Light microscopic examination of tumor tissues exhibited the connective tissue decreased by LPS and LPS+CR treated animals. The organization and amount of connective tissue matrix are directly related to tumor behavior, such as cancer cell migration and proliferation. Numerous solid tumors exhibit elevated expressions of extracellular matrix (ECM) components, including fibrillar collagens, elastin, laminins, and fibronectin. The source of these ECM molecules is tumor cells, but more often, cancer-associated fibroblasts. Indeed, infiltration of fibroblasts/myofibroblasts and subsequent accumulation of substantial amounts of collagenous ECM is observed in many solid tumors [38]. This process, called desmoplasia, is strongly associated with poor prognosis and resistance to systemic therapy. Therefore, the decrease in connective tissue in the treatment group is noteworthy and shows the contribution of the applied treatments to regulating the tumor microenvironment.

In order to understand the mechanisms underlying the effects of LPS and CR, NF – κB, JNK, and IL-6 levels were investigated in tumor tissues. NF-κB, an ancient protein transcription factor [39], is considered a regulator of innate immunity [40]. The NF-κB signaling pathway regulates cellular resistance against invading pathogens by linking pathogenic and cellular danger signals. Tumor tissue examination showed that NF-κB mRNA expressions were similar in the P and P+LPS groups. In contrast, the expression level increased in the P+LPS+CR group compared to the P and P+LPS groups. Besides the increased NF-κB expression level, IL-6, a proinflammatory cytokine, was also detected at higher levels in the P+LPS+CR group than in the other groups. In that respect, LPS alone administration was insufficient to trigger the NF-kB pathway. However, LPS+CR significantly activates NF-κB, which is the surviving and inflammatory pathway, has a curative effect, and is essential in suppressing tumor development in PDAC. In addition, mRNA expression levels of the JNK signaling pathway were determined in the tumor tissue. JNK is one of the central signaling cascades of the MAPK signaling pathway and is involved in apoptotic and non-apoptotic cell death mechanisms [41]. When JNK expression levels were evaluated between the groups, an increase was seen in the P+LPS group than in the P group and the P+LPS+CR group than in the P and P+LPS groups. However, considering that NF-κB is associated not only with inflammation but also with survival, JNK is directly associated with cell death, and IL-6 has immune regulatory properties other than inflammation, the mRNA expression results are quite significant, and LPS+CR explains the healing effect of its treatment on pancreatic tumor. Although LPS treatment alone was insufficient, it became effective in combination with 40% CR. In this case, it could be said that LPS applied to mice acts

http://doi.org/10.5472/marumj.1627620
Marmara Med J 2025;38(1): 15-23

through the JNK signaling besides the NF – κB pathway, and CR applied alongside LPS increases this effect and results in tumor shrinkage. This outcome may be attributed to CR's ability to reduce the availability of essential substrates and growth factors for cancer cells and regulate the tumor microenvironment and inflammation, thereby facilitating the delivery and efficacy of administered drugs.

Certain factors mentioned earlier that contribute to the increased occurrence of pancreatic cancer are also linked to the overproduction of ROS [42]. ROS are generated as a result of oxidative stress activation and have been observed in various cancer types due to their increased metabolic activities. If antioxidants do not inactivate ROS, they damage DNA, proteins, and lipids and produce several toxic and highly mutagenic metabolites that can alter tumor behavior and turn it into a malignant phenotype. To ensure survival, cancer cells can regulate ROS levels and prevent cell death [43]. Regarding oxidative stress, researchers revealed in the study that ROS levels in LPS-stimulated pancreatic acinar cells increased via the TLR4/NF-κB pathway and cell viability decreased with increased stress [44]. In this study, after subcutaneous PDAC tumors were removed, oxidative stress markers and antioxidant enzyme levels were measured. According to results, it was found that CR increased the GSH level and SOD activity, although not significantly, while LPS slightly increased the CAT activity and decreased the PCO level. We understand from these results that the effect pathways of LPS and CR in terms of ROS and antioxidant system on pancreatic tumors are different. Based on the recent knowledge, considering the dual roles, it is suggested that the treatment protocols to decrease or increase ROS could be effective in pancreatic cancer therapy. Our study showed that the anti-tumoral effects of low-dose LPS and CR combination are independent of the changing balance of the ROS and antioxidant levels.

Conclusion

This study aimed to explore how the combined impact of low-dose LPS treatment and CR influences the tumor microenvironment in PDAC. It was found that the applied treatment resulted in a reduction in tumor size and mass. LPS treatment alone did not produce the expected therapeutic effect, but with CR administration, induction of NF-κB, JNK, and IL-6 pathways increased, and tumor growth and development were inhibited. Histological examinations revealed that the stroma in the tumor decreased with the application of CR. In this context, further studies need to elucidate the effects of CR and/or LPS application on the tumor microenvironment. The results provide insight into developing new treatment options for PDAC.

Acknowledgments

The authors would like to thank Dr. Christine Hackbarth and Dr. Lars Ivo Partecke from the Department of Surgery, the University of Greifswald, Germany for the generous donation of Panc02 cells.

Compliance with Ethical Standards

Ethical approval: Required ethical approvals were given by the Bezmialem Foundation University, Laboratory Animals Local Ethics Committee (Project number 2017/190, Istanbul, Turkey). All mice were kept in standard conditions according to the Regulation of Animal Research Ethics in Turkey.

Conflict of interest: The authors declare that there is no conflict of interest.

Financial support: This research was funded by a grant from Istanbul University-Cerrahpasa, Scientific Research Projects Unit (Project No: 25597).

Authors contributions: ABB: Conception and design of the study, acquisition, analysis, and interpretation of data, drafting the manuscript, BI: Acquisition, analysis and interpretation of data, drafting the manuscript, ZMCY and MK: Analysis and interpretation of data, revising the manuscript critically for important intellectual content, SB: Conception and design of the study, analysis and interpretation of data, revising the manuscript critically for important intellectual content. All authors approved the final version of the manuscript.

REFERENCES

[1] Siegel RL, Miller KD, Fuchs HE, Jemal A. Cancer Statistics, 2021. CA Cancer J Clin 2021; 71:7-33. doi: 10.3322/caac.21654.

[2] Li C, Cui L, Yang L, et al. Pancreatic stellate cells promote tumor progression by promoting an ımmunosuppressive microenvironment in murine models of pancreatic cancer. Pancreas 2020;49:120-7. doi: 10.1097/MPA.000.000.0000001464.

[3] Chandana SR, Babiker HM, Mahadevan D. Therapeutic trends in pancreatic ductal adenocarcinoma (PDAC). Expert Opin Investig Drugs 2019;28:161-77. doi: 10.1080/13543.784.2019.1557145.

[4] Alexander C, Rietschel ET. Bacterial lipopolysaccharides and innate immunity. J Endotoxin Res 2001;7: 167-202. doi: 10.1179/096.805.101101532675.

[5] Wu TT, Chen TL, Chen RM. Lipopolysaccharide triggers macrophage activation of inflammatory cytokine expression, chemotaxis, phagocytosis, and oxidative ability via a toll-like receptor 4-dependent pathway: Validated by RNA interference. Toxicol Lett 2009;191:195-202. doi: 10.1016/j.toxlet.2009.08.025.

[6] Fang H, Pengal RA, Cao X, et al. Lipopolysaccharide-induced macrophage inflammatory response is regulated by SHIP. J Immunol 2004;173:360-6. doi: 10.4049/jimmunol.173.1.360.

[7] Seeley JJ, Ghosh S. Molecular mechanisms of innate memory and tolerance to LPS. J Leukoc Biol 2017;101:107-19. doi: 10.1189/jlb.3mr0316-118rr.

[8] Lashinger LM, Malone LM, Brown GW, et al. Rapamycin partially mimics the anticancer effects of calorie restriction in a murine model of pancreatic cancer. Cancer Prev Res 2011;4:1041-51. doi: 10.1158/1940-6207.CAPR-11-0023.

[9] O'Flanagan CH, Smith LA, McDonell SB, et al. When less may be more: Calorie restriction and response to cancer therapy. BMC Med 2017;15: 106. doi: 10.1186/s12916.017.0873-x.

[10] Vidoni C, Ferraresi A, Esposito A, et al. Calorie restriction for cancer prevention and therapy: mechanisms, expectations, and efficacy. J Cancer Prev 2021;26:224-36. doi: 10.15430/jcp.2021.26.4.224.

[11] Meynet O, Ricci JE. Caloric restriction and cancer: Molecular mechanisms and clinical implications. Trends Mol Med 2014;20:419-27. doi: 10.1016/j.molmed.2014.05.001.

[12] Lu Y, Tao F, Zhou MT, Tang KF. The signaling pathways that mediate the anti-cancer effects of caloric restriction. Pharmacol Res 2019;141:512-20. doi: 10.1016/j.phrs.2019.01.021.

[13] Lee C, Raffaghello L, Brandhorst S, et al. Fasting cycles retard growth of tumors and sensitize a range of cancer cell types to chemotherapy. Sci Transl Med 2012,4:124ra27. doi: 10.1126/scitranslmed.3003293.

[14] Lanza-Jacoby S, Yan G, Radice G, LePhong C, Baliff J, Hess R. Calorie restriction delays the progression of lesions to pancreatic cancer in the LSL-KrasG12D; Pdx-1/Cre mouse model of pancreatic cancer. Exp Biol Med 2013,238:787-97. doi: 10.1177/153.537.0213493727.

[15] Ekiz-Yilmaz T, Isildar B, Gezer A, et al. The role of unfolded protein response in the pathogenesis of endometriosis: contribution of peritoneal fluid. Reprod Biomed Online 2021,42:1-15. doi: 10.1016/j.rbmo.2020.09.012.

[16] Sarantis P, Koustas E, Papadimitropoulou A, et al. Pancreatic ductal adenocarcinoma: Treatment hurdles, tumor microenvironment and immunotherapy. World J Gastrointest Oncol 2020,12:173-81. doi: 10.4251/wjgo.v12.i2.173.

[17] Beydogan AB, Coskun Yazici ZM, Bolkent S. Influences of calorie restriction and lipopolysaccharide therapy on inflammation, cytokine response, and cell proliferation in pancreatic adenocarcinoma mouse model. J Biochem Mol Toxicol 2023;37:1-10. doi: 10.1002/jbt.23250.

[18] Green CL, Mitchell SE, Derous D, et al. The effects of graded levels of calorie restriction: IX. Global metabolomic screen reveals modulation of carnitines, sphingolipids and bile acids in the liver of C57BL/6 mice. Aging Cell 2017;16:529-40. doi: 10.1111/acel.12570.

[19] Bradford MM. A rapid and sensitive method for the quantitation of microgram quantities of protein utilizing the principle of protein-dye binding. Anal Biochem 1976;72:248-54. doi: 10.1016/0003-2697(76)90527-3.

[20] Aebi H. Catalase in vitro. Methods Enzymol 1984;105:121-6. doi: 10.1016/S0076-6879(84)05016-3.

[21] Ledwozyw A, Michalak J, Stępień A, Kadziolka A. The relationship between plasma triglycerides, cholesterol, total lipids and lipid peroxidation products during human atherosclerosis. Clin Chim Acta 1986,155:275-83. doı: 10.1016/0009-8981(86)90247-0.

[22] Beutler E, Duron O, Kelly BM. Improved method for the determination of blood glutathione. J Lab Clin Med 1963;61:882-8.

[23] Sun Y, Oberley LW, Li Y. A simple method for clinical assay of superoxide dismutase. Clin Chem 1988;34:497-500. doi: 10.1093/clinchem/34.3.497.

[24] Reznick AZ, Packer L. Oxidative damage to proteins: Spectrophotometric method for carbonyl assay. Methods Enzymol 1994;233:357-63. doi: 10.1016/S0076-6879(94)33041-7.

[25] Honda T, Inagawa H. Molecular response of human monocytes following interaction with colon cancer cells by pre-treatment with low-dose lipopolysaccharide. Anticancer Res 2015;35:4473-7.

[26] Raza H, John A, Shafarin J. Potentiation of LPS-induced apoptotic cell death in human hepatoma HepG2 cells by aspirin via ROS and mitochondrial dysfunction: Protection by N-acetyl cysteine. PLoS One 2016;11:e0157750. doi: 10.1371/journal.pone.0159750.

[27] Honda T, Inagawa H. Usefulness of monocytes/macrophages activated with low-dose lipopolysaccharide in tumor tissue and adipose tissue of obesity. Anticancer Res 2019;39:4475-8. doi: 10.21873/anticanres.13621.

[28] Brooks D, Barr LC, Wiscombe S, Mcauley DF, Simpson AJ, Rostrron AJ. Human lipopolysaccharide models provide mechanistic and therapeutic insights into systemic and pulmonary inflammation. Eur Respir J 2020;56:1901298. doi: 10.1183/13993.003.01298-2019.

[29] Millischer V, Heinzl M, Faka A, et al. Intravenous administration of LPS activates the kynurenine pathway in healthy male human subjects: a prospective placebo-controlled cross-over trial. J Neuroinflammation 2021;18:158. doi: 10.1186/s12974.021.02196-x.

[30] Buters TP, Hameeteman PW, Jansen IME, et al. Intradermal lipopolysaccharide challenge as an acute in vivo inflammatory model in healthy volunteers. Br J Clin Pharmacol 2022;88:680-90. doi: 10.1111/bcp.14999.

[31] Larsson J, Hoppe E, Gautrois M, Cvijovic M, Jirstrand M. Optimizing study design in LPS challenge studies for quantifying drug induced inhibition of TNFα response: Did we miss the prime time? Eur J Pharm Sci 2022;176:106256. doi: 10.1016/j.ejps.2022.106256.

[32] Lien EC, Westermark AM, Li Z, Sapp K M, Heiden M G V.Caloric restriction alters lipid metabolism to contribute to tumor growth inhibition. bioRxiv Epub ahead of print 2020. doi: 10.1101/2020.03.09.984302.

[33] Lashinger LM, Harrison LM, Rasmussen AJ, et al. Dietary energy balance Heidenmodulation of Kras – and Ink4a/Arf +/—driven pancreatic cancer: The role of insulin-like growth factor-I. Cancer Prev Res (Phila) 2013;6:1046-55. doi: 10.1158/1940-6207.CAPR-13-0185.

[34] Brandhorst S, Longo VD. Fasting and caloric restriction in cancer prevention and treatment. Recent Results Cancer Res 2016;207:241-66. .doi: 10.1007/978-3-319-42118-6_12.

[35] Sadeghian M, Rahmani S, Khalesi S, Hejazi E. A review of fasting effects on the response of cancer to chemotherapy. Clin Nutr 2021;40:1669-81. doi: 10.1016/j.clnu.2020.10.037.

[36] Jain S, Dash P, Minz AP, et al. Lipopolysaccharide (LPS) enhances prostate cancer metastasis potentially through NF-κB activation and recurrent dexamethasone administration fails

to suppress it in vivo. Prostate 2019.79:168-82. doi: 10.1002/pros.23722.

[37] Jiang Y, Ji X, Liu K, et al. Exosomal miR-200c-3p negatively regulates the migraion and invasion of lipopolysaccharide (LPS)-stimulated colorectal cancer (CRC). BMC Mol Cell Biol 2020;21:48. doi: 10.1186/s12860.020.00291-0.

[38] Henke E, Nandigama R, Ergün S. Extracellular matrix in the tumor microenvironment and its impact on cancer therapy. Front Mol Biosci 2020;6:160. . doi: 10.3389/fmolb.2019.00160.

[39] Salminen A, Huuskonen J, Ojala J, Kauppinen A, Kaarniranta K, Suuronen T. Activation of innate immunity system during aging: NF-kB signaling is the molecular culprit of inflamm-aging. Ageing Res Rev 2008;7:83-105. doi: 10.1016/j.arr.2007.09.002.

[40] Baltimore D. Discovering NF-kappaB. Cold Spring Harb Perspect Biol 2009;1:a000026. doi: 10.1101/cshperspect.a000026.

[41] Yarza R, Vela S, Solas M, Ramirez M J. c-Jun N-terminal kinase (JNK) signaling as a therapeutic target for Alzheimer's disease. Front Pharmacol 2016;6:321. doi: 10.3389/fphar.2015.00321.

[42] Nöthlings U, Wilkens LR, Murphy SP, Hankin J H, Henderson M E, Kolonel L N.Meat and fat intake as risk factors for pancreatic cancer: The multiethnic cohort study. J Natl Cancer Inst 2005;97:1458-65. doi: 10.1093/jnci/dji292.

[43] Martinez-Useros J, Li W, Cabeza-Morales M, Foncillas J G. Oxidative stress: A new target for pancreatic cancer prognosis and treatment. J Clin Med 2017;6:29. doi: 10.3390/jcm6030029.

[44] Pan L, Yu L, Wang L, et al. Inflammatory stimuli promote oxidative stress in pancreatic acinar cells via Toll-like receptor 4/nuclear factor-κB pathway. Int J Mol Med 2018;42:3582-90. doi: 10.3892/ijmm.2018.3906.